

Supporting Information

Strain Stiffening Hydrogels through Self-Assembly and Covalent Fixation of Semi-Flexible Fibers

*Marcos Fernandez-Castano Romera, René P. M. Lafleur, Clément Guibert, Ilja K. Voets, Cornelis Storm, and Rint P. Sijbesma**

anie_201704046_sm_miscellaneous_information.pdf

Table of contents

1. Materials	2
2. General methods	2
3. Synthetic procedures.....	4
4. Contour and persistence length calculation	11
5. UV-Vis spectrum of DA.....	12
6. Calculation of number of ribbons per fiber	13
7. Gel preparation method	16
8. Effect of Cu^{I} ions on gelation process	17
9. Scaling relationships.....	18
10. References.....	20

1. Materials

All solvents used were of reagent grade quality or better and purchased from Biosolve, Sigma-Aldrich or Actu-All Chemicals. THF and DCM were dried using molecular sieves (3 Å). All chemicals were purchased from Sigma-Aldrich, TCI Europe, Acros or Fluka at the highest purity available and used without further purification unless otherwise stated. Flash chromatography was performed on a Reveleris X2 system using 40µm mesh silica gel cartridges. Reactions were followed by thin-layer chromatography (precoated 0.25 mm, 60-F254 silica plate purchased from Merck). Tetraethylene glycol monopropargyl ether (**1**), azido-tetraethylene glycol (**2**),^[1] N-(*tert*butyloxycarbonyl)-11-aminoundecanoic acid (Boc-AUDA),^[2] 1,12-diisocyanatodeca-4,6-diyne,^[3] and **DA** were prepared according to literature procedures.

2. General methods

NMR spectra were recorded on a 400 MHz Varian Mercury Vx (100 MHz for ¹³C-NMR) or 400 MHz Bruker UltraShield Magnet (100 MHz for ¹³C-NMR). Chemical shifts (δ) are reported in parts per million (ppm) using residual solvent signal or tetramethylsilane (TMS) as internal standards.^[4] Splitting patterns are labeled as singlet (s), doublet (d), double doublet (dd), triplet (t), quartet (q), pentet (p) and multiplet (m). Infrared spectra were measured on a Perkin Elmer 1600FT-IR equipped with a Perkin Elmer Universal ATR Sampler Accessory. Matrix assisted laser desorption ionization time-of-flight (MALDI-TOF) measurements were carried out on a Perseptive DE PRO Voyager mass spectrometer using α-cyano-4-hydroxycinnamic acid as the calibration matrix. (LC-MS).

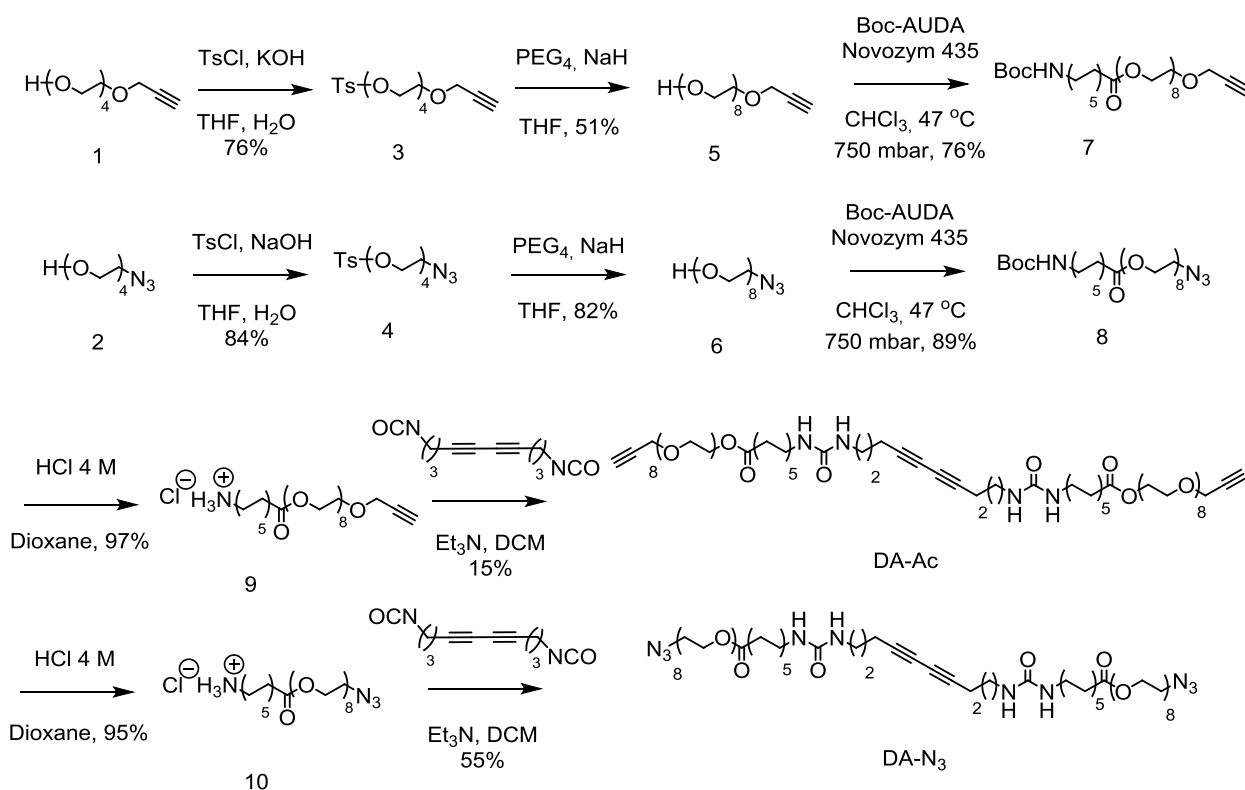
Cryo-TEM micrographs were obtained in ‘Vitrobot’ instrument (PC controlled vitrification robot, patent applied, Frederik *et al.* 2002, patent licensed to FEI) at room temperature and relative humidity >95%. In the preparation chamber of the ‘Vibrobot’, 3 µL sample were dropped on a Quantifoil grid (R 2/2, Quantifoil Micro Tools GmbH; freshly glow discharged just prior use), the excess of liquid was blotted away for 2 s and -2 mm and the so-formed film was shot (acceleration about 3g) into liquid ethane. The vitrified film was transferred to a cryoholder (Gatan 626) and observed at -170 °C in a Tecnai Sphera microscope operating at 200 kV. Micrographs were taken at low dose conditions.

Small angle X-Ray scattering (SAXS) profiles were recorded on SAXLAB GANESHA 300 XL SAXS equipped with a GeniX 3D Cu Ultra Low Divergence micro focus sealed tube source producing X-rays with a wavelength λ=1.54 Å at a flux of 1×10⁸ ph/s and a Pilatus 300 K silicon pixel detector with 487 × 619 pixels of 172 × 172 µm² in size placed a three sample-to-detector distances of 113, 713, and 1513 mm respectively to cover a q-range of 0.07 ≤ q ≤ 3.0 nm⁻¹ with q = 4π/λ(sin θ/2). Silver behenate was used for calibration of the beam center as well as the q-range. Samples were measured within 2 mm quartz capillaries (Hilgenberg GmbH, Germany). The two-dimensional SAXS patterns were brought to an absolute intensity scale using the calibrated detector response function, known sample-to-detector distance, measured incident and transmitted beam intensities, and azimuthally averaged to obtain one dimensional SAXS profiles. The scattering curves of the fibers were obtained by subtraction of the scattering contribution of the solvent and quartz cell.

The mechanical properties of the hydrogels were tested by oscillatory rheology. Dynamic viscoelastic measurements were conducted on a stress-controlled Anton Paar, Physicia MCR 501 rheometer equipped with a 25-mm stainless steel sand-blasted plate-plate geometry to prevent slippage of the sample. Measurements were performed at a fixed temperature of 20 °C sealed by placing mineral oil around the sample to minimize evaporation at a fixed plate-to-plate gap of 800 µm. After addition of

the catalyst, gelation was monitored by continuous oscillations with a strain amplitude of 0.1 % and an angular frequency of 6.28 rad/s. To probe the elasticity of the gels, we applied a steady prestress, σ_0 on which a oscillatory stress, $\delta\sigma(t) = \delta\sigma e^{i\omega t}$ is superimposed with an amplitude at most 10% of σ_0 and at an angular frequency of $\omega = 6.28 \text{ rad s}^{-1}$.

3. Synthetic procedures



Scheme S1. Synthetic route towards **DA-Ac** and **DA-N₃** analogues.

Tetraethylene glycol monopropargyl ether tosylate (3)

Tetraethylene glycol monopropargyl ether (**1**) (12.85 g, 55.35 mmol), tosyl chloride (12.63 g, 66.24 mmol) and THF (250 mL) were placed in a round bottomed flask and the mixture was chilled in an ice bath. At this temperature, an aqueous solution of KOH 16 M (12.54 g, 0.22 mol) was added dropwise and the reaction mixture was allowed to stir overnight at room temperature. At the conclusion of the reaction, the mixture was poured into ice H₂O (150 mL) and the aqueous layer extracted trice with DCM (150 mL). The organic extracts were combined and washed twice with 3% HCl (150 mL) and once with brine (150 mL), dried over MgSO₄ and concentrated under reduced pressure. The resultant crude product was purified by flash chromatography (silica gel, DCM/EtOH, 99:1 v/v) to yield **3** (16.31 g, 42.24 mmol, 76%) as a faint yellow oil.

¹H-NMR (400 MHz, CDCl₃, T=295K): δ = 7.76 (d, 2H, J=8.0 Hz, Ar), 7.31 (d, 2H, J=8.0 Hz, Ar), 4.16 (d, 2H, J=2.4 Hz, CH₂C≡H), 4.13 (t, 2H, J=4.0 Hz, CH₂tosyl), 3.66-3.55 (m, 14H, CH₂O), 2.41 (m, 4H, tosylCH₃ + CH₂C≡H).

¹³C-NMR (400 MHz, CDCl₃, T=295K): δ = 144.84, 133.02, 129.86, 127.99, 79.70, 74.61, 70.74-70.41, 69.31, 69.13, 68.69, 58.41, 21.67.

MALDI-TOF-MS: calculated Mw=386.14 g/mol, found m/z [M+Na⁺] = 409.33, m/z [M+NH₄⁺] = 404.25, [M+H⁺] = 387.17.

Azido-tetraethylene glycol tosylate (4)

Azido-tetraethylene glycol (**2**) (6.84 g, 31.21 mmol), tosyl chloride (6.70 g, 35.16 mmol) and THF (140 mL) were placed in a round bottomed flask and the mixture was cooled to 0 °C in an ice bath. At this temperature, an aqueous solution of NaOH 4.8 M (4.81 g, 0.12 mol) was added dropwise and the reaction mixture was stirred overnight at room temperature. At the conclusion of the reaction, the mixture was chilled in an ice bath and quenched with HCl 1M (150 mL). The organic layer was removed by rotary evaporation and the remaining aqueous solution extracted thrice with DCM (150 mL). The organic extracts were combined and washed twice with 10% Na₂CO₃ (150 mL), H₂O (150 mL) and dried over MgSO₄. The final product was evaporated to dryness to afford **4** (9.76g, 26.16 mmol, 84%) which was used in subsequent steps without further purification.

¹H-NMR (400 MHz, CDCl₃, T=295K): δ = 7.76 (d, 2H, J=8.4 Hz, Ar), 7.32 (d, 2H, J=8.4 Hz, Ar), 4.14 (t, 2H, J=4.7 Hz, CH₂tosyl), 3.68-3.57 (m, 12H, CH₂O), 3.36 (t, 2H, J=5.2 Hz, CH₂N₃), 2.43 (s, 3H, tosylCH₃).

¹³C-NMR (400 MHz, CDCl₃, T=295K): δ = 144.89, 133.05, 129.89, 128.02, 70.80-70.65, 70.09, 69.33, 68.73, 50.74, 21.70.

MALDI-TOF-MS: calculated Mw=373.13 g/mol, found m/z [M+Na⁺] = 396.25, m/z [M+NH₄⁺] = 391.17, [M+H⁺] = 373.92.

Octaethylene glycol monopropargyl ether (**5**)

Tetraethylene glycol (PEG₄) (48.97 g, 0.253 mol) in anhyd. THF (200 mL) was placed in a round-bottom flask and chilled in an ice bath under atmosphere of argon. To the resultant solution, sodium hydride (NaH) (60% dispersion in mineral oil, 2.65 g, 66.34 mmol) was added in three portions over a period of 30 mins and the reaction mixture was allowed to warm to r.t. followed by the addition of **3** (16.31 g, 42.24 mmol) in dry THF (10 mL) by syringe pump over 7h. The reaction mixture was further stirred for 2d under atmosphere of argon. At the conclusion of the reaction, brine (150 mL) was added and to quench the excess of NaH and the organic layer was evaporated under reduced pressure. The resultant aqueous slurry was extracted thrice with CH₂Cl₂ (150 mL) and the combined organic extracts were collected, washed with 10 wt% aqueous solution of KHPO₄ (150 mL), H₂O (150 mL), dried over anhyd. MgSO₄ and concentrated *in vacuo*. The crude product was subjected to flash column chromatography (silica gel, DCM/EtOH 97:3 v/v) to afford **5** (8.80 g, 21.56 mmol, 51%) as a faint yellow viscous oil.

¹H-NMR (400 MHz, CDCl₃, T=295K): δ = 4.19 (d, 2H, J=3.2 Hz, CH₂C≡CH), 3.64-3.51 (m, 32H, CH₂O), 2.40 (t, 1H, J=2.4 Hz, C≡CH).

¹³C-NMR (400 MHz, CDCl₃, T=295K): δ = 79.59, 74.60, 72.48, 70.51-70.45, 70.31, 70.25, 69.00, 61.56, 58.30.

MALDI-TOF-MS: calculated Mw=408.28 g/mol, found m/z [M+Na⁺] = 431.50, m/z [M+H⁺] = 409.42.

Azido-octaethylene glycol (**6**)

4 (9.76 g, 26.16 mmol) was reacted following the same procedure as described for **5**. The crude product obtained after liquid-liquid extraction was subjected to column chromatography (silica gel, gradients DCM/EtOH, 99:1 to 19:1 v/v) to yield **6** (8.53 g, 21.58 mmol, 82%) as a faint yellow viscous oil.

$^1\text{H-NMR}$ (400 MHz, CDCl_3 , T=295K): δ = 3.69-3.65 (m, 30H, CH_2O), 3.39 (t, 2H, J=4.0 Hz, CH_2N_3).

$^{13}\text{C-NMR}$ (400 MHz, CDCl_3 , T=295K): δ = 72.42, 70.49-70.35, 70.14, 69.86, 61.44, 50.48.

MALDI-TOF-MS: calculated Mw=395.23 g/mol, found m/z $[\text{M}+\text{Na}^+]$ = 418.42, m/z $[\text{M}+\text{H}^+]$ = 396.33.

N-(tert-butyloxycarbonyl)-11-aminoundecanoyl-(octaethyleneglycol monopropargyl ether)-ester (7)

N-(tertbutyloxycarbonyl)-11-aminoundecanoic acid (Boc-AUDA) (4.45 g, 14.76 mmol), **5** (5.05 g, 12.37 mmol) and Novozym 435 (2.85 g, 30 wt%) in CHCl_3 (50 mL) were placed in a round bottom flask and the reaction mixture was stirred at 47 °C and 750 mbar in a rotavap apparatus for 5h. To the resultant solution, molecular sieves were added and the mixture was allowed to react overnight. The suspension was filtered off, and the filtrate dried by rotary evaporation. The product was purified using flash column chromatography (silica gel, CH_2Cl_2 /Ethanol 23:2 v/v) yielding **7** (6.49 g, 9.386 mmol, 76%) as a viscous colourless oil.

$^1\text{H-NMR}$ (400 MHz, CDCl_3 , T=295K): δ = 4.60 (bs, 1H, NH), 4.12 (t, 2H, J = 4.76 Hz, CH_2OCO), 4.10 (d, 2H, J=2.4 Hz, $\text{CH}_2\text{C}\equiv\text{CH}$), 3.60-3.56 (m, 30H, OCH_2), 2.99 (q, 2H, J = 6.48 Hz, CH_2N), 2.38 (t, 1H, J=2.36 Hz, $\text{C}\equiv\text{CH}$), 2.23 (t, 2H, J=7.48 Hz $\text{CH}_2\text{-CO}$) 1.56-1.47 (m, 2H, $\text{CH}_2\text{CH}_2\text{CO}$), 1.34 (s, 9H, $\text{C}(\text{CH}_3)_3$), 1.24-1.13 (m, 14H, CH_2).

$^{13}\text{C-NMR}$ (400 MHz, CDCl_3 , T=295K): δ = 173.64, 155.87, 79.53, 78.71, 74.57, 70.49-70.42, 70.28, 69.06, 68.96, 63.24, 58.26, 40.48, 34.05, 29.95, 29.35-28.97, 28.34, 26.67, 24.76.

MALDI-TOF-MS: calculated Mw=691.45 g/mol, found m/z $[\text{M}+\text{Na}^+]$ = 714.47.

N-(tert-butyloxycarbonyl)-11-aminoundecanoyl-(azido-octaethyleneglycol)-ester (8)

6 (4.00 g, 10.12 mmol) was reacted following the same experimental procedure as described for **7** to give **8** (6.15 g, 9.06 mmol, 89%) as a transparent oil.

$^1\text{H-NMR}$ (400 MHz, CDCl_3 , T=295K): δ = 4.54 (bs, 1H, NH), 4.12 (t, 2H, J = 4.80 Hz, CH_2OCO), 3.66-3.61 (m, 30H, OCH_2), 3.55 (t, 2H, J=5.24 Hz, CH_2N_3), 3.05 (q, 2H, J = 6.20 Hz, CH_2N), 2.28 (t, 2H, J=7.48 Hz CH_2CO), 1.64-1.50 (m, 2H, $\text{CH}_2\text{CH}_2\text{CO}$), 1.40 (s, 9H, $\text{C}(\text{CH}_3)_3$), 1.32-1.15 (m, 14H, CH_2).

$^{13}\text{C-NMR}$ (400 MHz, CDCl_3 , T=295K): δ = 173.75, 155.95, 78.85, 70.64-70.50, 70.00, 69.14, 63.32, 50.62, 40.56, 34.13, 30.01, 29.42-29.05, 28.40, 26.74, 24.84.

MALDI-TOF-MS: calculated Mw=678.44 g/mol, found m/z $[\text{M}+\text{Na}^+]$ = 701.44.

11-aminoundecanoyl-(octaethyleneglycol monopropargyl ether)-ester-HCl salt (9)

A solution of HCl 4 M in dioxane (35 mL) was cooled to 0 °C in an ice bath. At this temperature, **7** (6.49 g, 9.39 mmol) in dioxane (35 mL) was added dropwise under atmosphere of argon and the reaction mixture was stirred for 4 hours at r.t. At the conclusion of the reaction, the volatiles were removed *in vacuo* and **9** (5.72 g, 9.12 mmol, 97%) was isolated as a faintly yellow waxy solid.

$^1\text{H-NMR}$ (400 MHz, CDCl_3 , T=295K): δ = 8.10 (bs, 3H, CH_2NH_3), 4.13-4.11 (m, 4H, $\text{CH}_2\text{C}\equiv\text{CH} + \text{CH}_2\text{OCO}$), 3.61-3.56 (m, 30H, OCH_2), 2.87 (m, 2H, CH_2NH_3), 2.39 (t, 1H, J=2.36 Hz, $\text{C}\equiv\text{CH}$), 2.22 (t, 2H, J =7.52 Hz, CH_2CO), 1.66 (m, 2H, CH_2NH_3), 1.51 (m, 2H, $\text{CH}_2\text{CH}_2\text{CO}$) 1.24-1.17 (m, 12H, CH_2).

$^{13}\text{C-NMR}$ (400 MHz, CDCl_3 , T=295K): δ = 173.33, 79.53, 74.66, 70.42-70.37, 70.22, 69.05, 68.91, 63.22, 58.28, 39.90, 34.05, 29.05-28.91, 27.44, 26.50, 24.75.

MALDI-TOF-MS: calculated Mw=591.78 g/mol, found m/z $[\text{M}+\text{H}^+] = 592.75$.

11-aminoundecanoyl-(azido-octaethyleneglycol)-ester-HCl salt (10)

8 (6.15 g, 9.06 mmol) was reacted following the same experimental procedure as described for **9** yielding **10** (5.26 g, 8.57 mmol, 95%) as a slightly yellow waxy solid.

$^1\text{H-NMR}$ (400 MHz, CDCl_3 , T=295K): δ = 8.12 (bs, 3H, CH_2NH_3), 4.17 (m, 2H, CH_2OCO), 3.66-3.61 (m, 28H, OCH_2), 3.55 (t, 2H, J=5.0 Hz, CH_2N_3), 2.92 (m, 2H, CH_2NH_3), 2.27 (t, 2H, J =7.52 Hz, CH_2CO), 1.71 (m, 2H, CH_2NH_3), 1.56 (m, 2H, $\text{CH}_2\text{CH}_2\text{CO}$) 1.31-1.22 (m, 12H, CH_2).

$^{13}\text{C-NMR}$ (400 MHz, CDCl_3 , T=295K): δ = 173.80, 70.66-70.53, 70.02, 69.31, 63.35, 50.68, 40.00, 34.18, 29.31-28.98, 27.61, 26.55, 24.87.

MALDI-TOF-MS: calculated Mw=578.75 g/mol, found m/z $[\text{M}+\text{Na}^+] = 601.50$, m/z $[\text{M}+\text{H}^+] = 579.75$.

DA-Ac

9 (1.98 g, 3.12 mmol), triethylamine (0.84 g, 8.33 mmol) and anhyd. CH_2Cl_2 (15 mL) were placed in a round bottomed flask under argon atmosphere and the mixture was cooled to 0 °C in an ice bath, followed by the dropwise addition of 1,12-diisocyanatodeca-4,6-diyne (0.31 g, 1.44 mmol) in dry CH_2Cl_2 (5 mL). The reaction was stirred for 1 hour at r.t, after which the crude product was concentrated under reduced pressure and purified using flash column chromatography (silica gel, $\text{CH}_2\text{Cl}_2/\text{Ethanol}$ 97:3 v/v) to afford **DA-Ac** (0.29 g, 0.21 mmol, 15%) as a white waxy solid that turned faintly pink under prolonged exposure to stray light.

$^1\text{H-NMR}$ (400 MHz, CDCl_3 , T=295K): δ = 5.04 (t, 2H, J=5.36 Hz, NH), 4.88 (t, 2H, J=4.84 Hz, NH), 4.21 (m, 8H, $\text{CH}_2\text{OCO} + \text{CH}_2\text{C}\equiv\text{H}$), 3.70-3.60 (m, 60H, OCH_2), 3.25 (q, 4H, J=6.24 Hz, CH_2NH), 3.11 (q, 4H, J=6.32 Hz, NHCH_2), 2.43 (t, 2H, J= 2.08 Hz, $\text{C}\equiv\text{CH}$), 2.31 (m, 8H, $\text{CH}_2\text{CO} + \text{CH}_2\text{C}\equiv\text{C}$), 1.69, (quint, 4H, J=6.68 Hz, $\text{NHCH}_2\text{CH}_2\text{CH}_2\text{CO}$), 1.60 (p, 4H, J=6.88 Hz, $\text{CH}_2\text{CH}_2\text{CO}$), 1.45 (p, 4H, J=6.32 Hz, $\text{CH}_2\text{CH}_2\text{NH}$), 1.30-1.25 (m, 24H, CH_2).

$^{13}\text{C-NMR}$ (400 MHz, CDCl_3 , T=295K): δ = 147.01, 158.77, 79.75, 74.71, 70.71-70.67, 70.51, 69.31, 69.21, 66.03, 63.49, 58.51, 40.55, 39.27, 34.31, 30.34, 29.57, 29.43, 29.30, 29.17, 28.15, 27.02, 24.99, 16.76.

MALDI-TOF-MS: calculated Mw=1398.89 g/mol, found m/z $[\text{M}+\text{Na}^+] = 1421.88$, m/z $[\text{M}+\text{K}^+] = 1437.86$.

FT-IR (ATR) ν (cm^{-1}): 3334, 2921, 2851, 1731, 1614, 1579, 1101, 621.

DA-N₃

10 (1.57 g, 2.56 mmol) was reacted following the same procedure as described for the synthesis of **DA-Ac** to yield **DA-N₃** (0.28 g, 0.20 mmol, 53%) as a white waxy solid that turned slightly purple under prolonged exposure to stray light.

¹H-NMR (400 MHz, CDCl₃, T=295K): δ = 5.01 (t, 2H, J=5.8 Hz, NH), 4.85 (t, 2H, J=5.48 Hz, NH), 4.85 (t, 4H, J= 4.8 Hz, CH₂OCO), 3.69-3.62 (m, 60H, OCH₂), 3.35 (t, 4H, J=5.24 Hz, CH₂N₃), 3.25 (q, 4H, J=6.2 Hz, CH₂NH), 3.12 (q, 4H, J=6.12 Hz, NHCH₂), 2.31 (m, 8H, CH₂CO+CH₂-C≡C), 1.69, (quint, 4H, J=6.72 Hz, NHCH₂CH₂CH₂CO), 1.60 (p, 4H, J=7.08 Hz, CH₂CH₂CO), 1.44 (p, 4H, J=6.56 Hz, CH₂CH₂NH), 1.31-1.25 (m, 24H, CH₂).

¹³C-NMR (400 MHz, CDCl₃, T=295K): δ = 174.01, 158.75, 70.81-70.68, 70.15, 69.31, 66.04, 63.49, 50.80, 40.57, 39.28, 34.31, 30.47, 29.57, 29.43, 29.31, 29.17, 28.90, 27.02, 24.99, 16.76.

MALDI-TOF-MS: calculated Mw=1372.87 g/mol, found m/z [M+Na⁺] = 1395.89, m/z [M+K⁺] = 1411.87.

FT-IR (ATR) ν (cm⁻¹): 3328, 2919, 2849, 2099, 1731, 1615, 1580, 1096, 608.

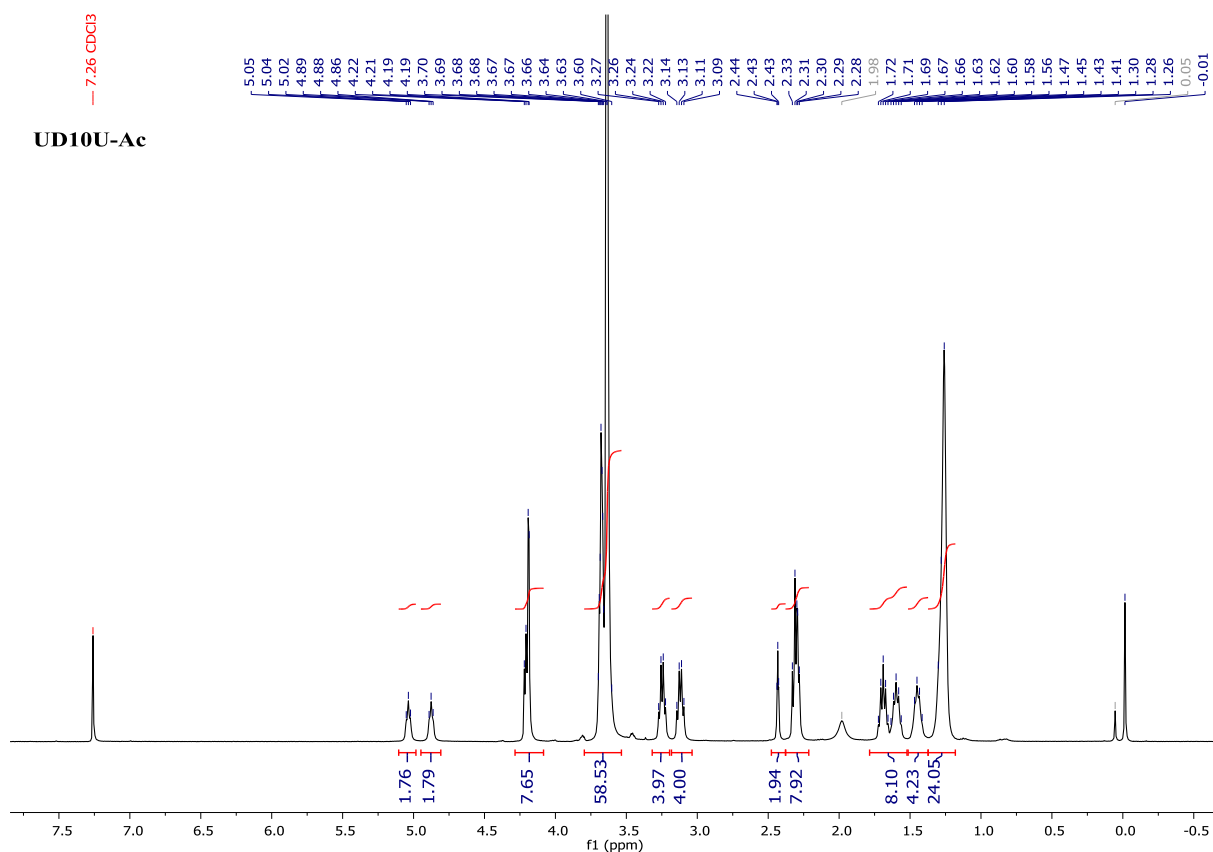


Figure S1. ¹H-NMR spectrum of DA-Ac.

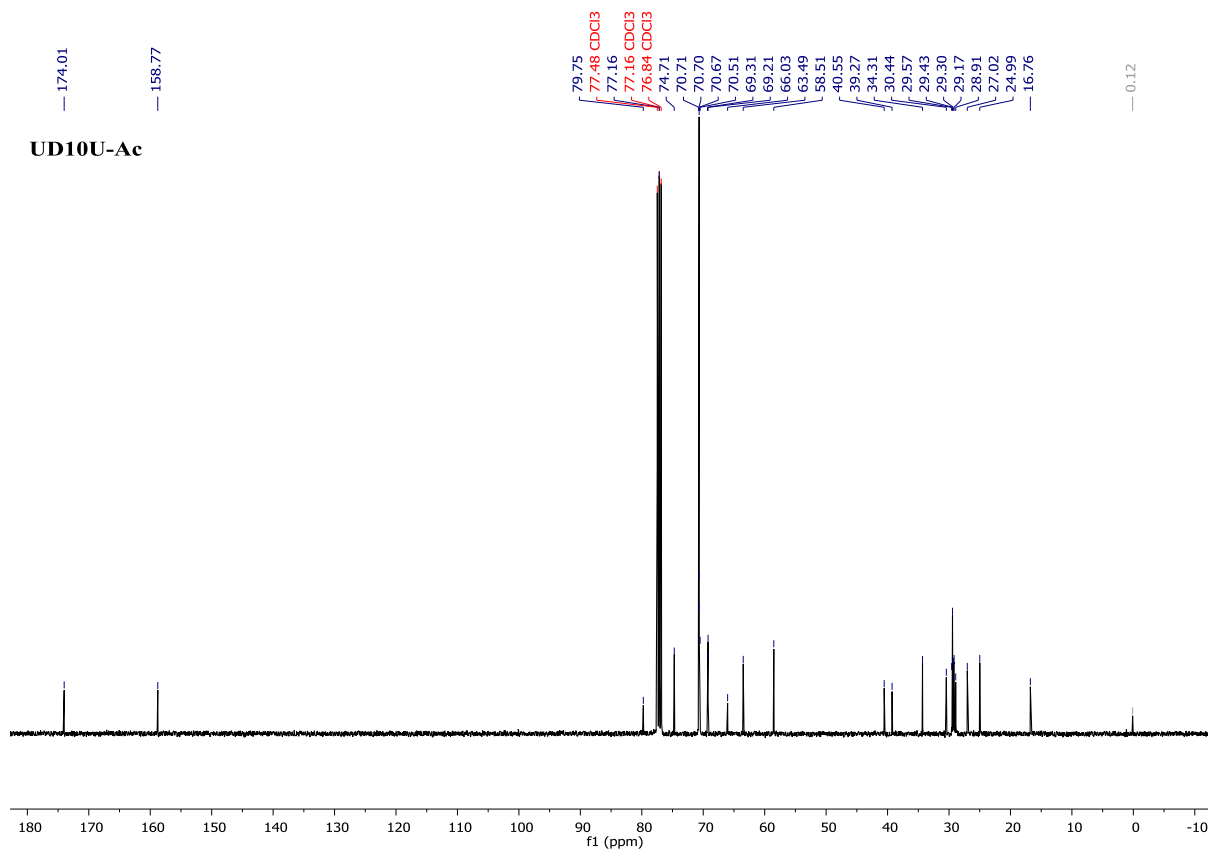


Figure S2. ^{13}C -NMR spectrum of DA-Ac.

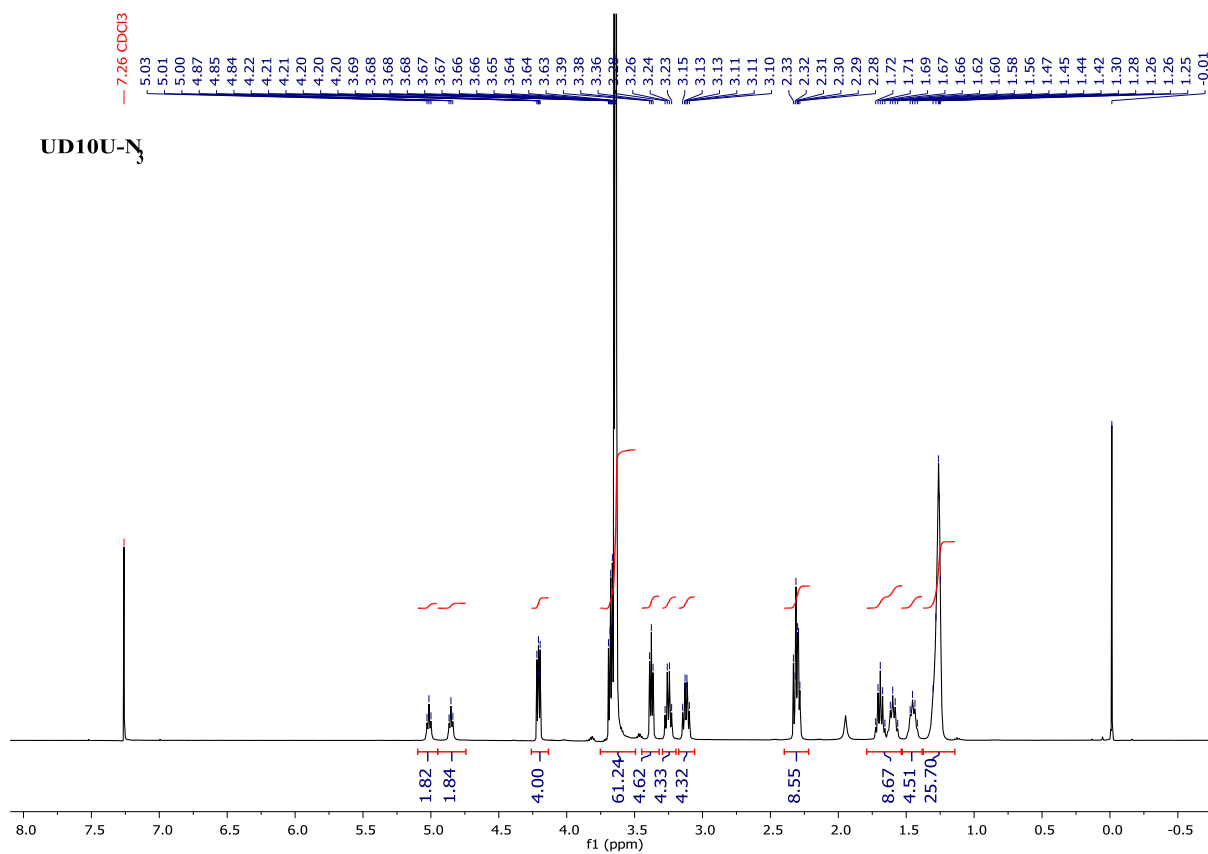


Figure S3. ^1H -NMR spectrum of DA-N₃.

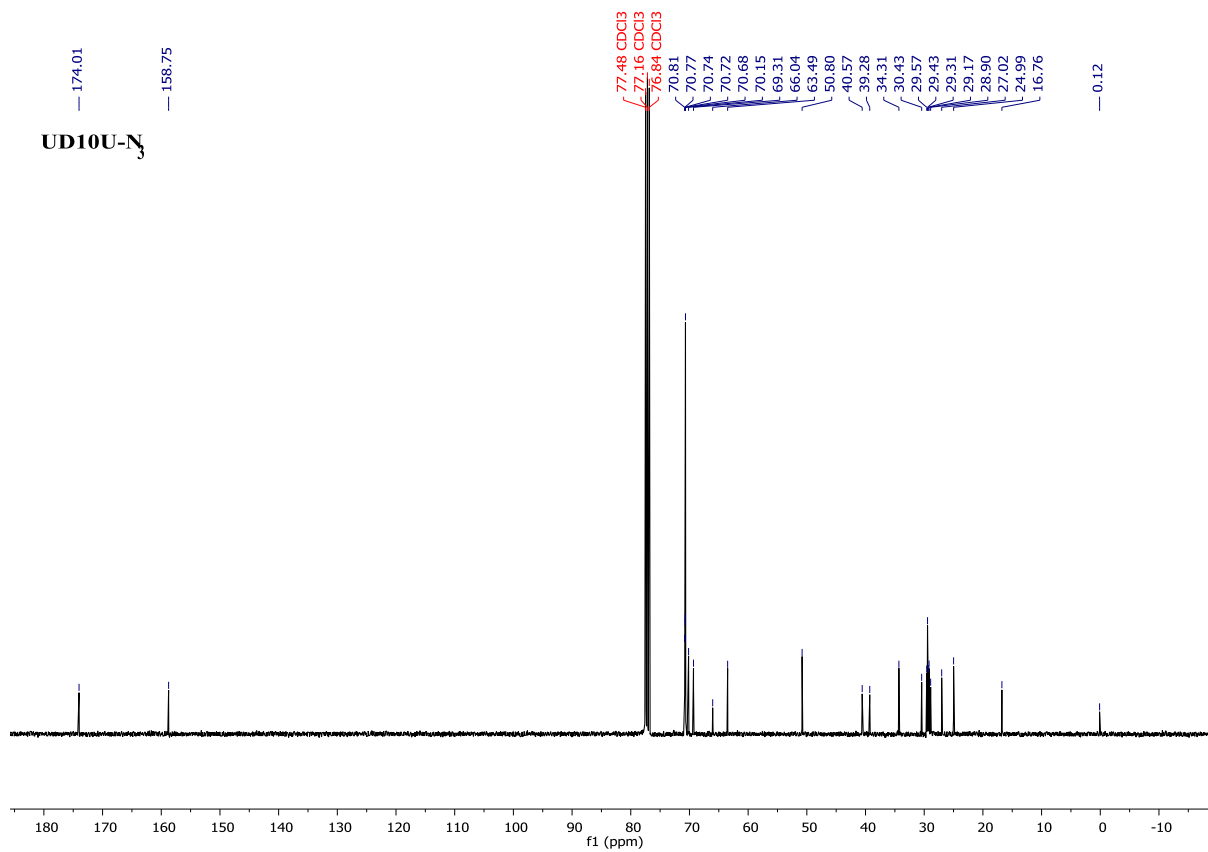


Figure S4. ¹³C-NMR spectrum of DA-N₃.

4. Contour and persistence length calculation

DA was weighed in the solid state and dissolved in ca. 300 μL chloroform. The solvent was allowed to evaporate overnight and the remaining solid was dissolved in mili-Q water to a concentration of 20 mg/mL. The micelles were allowed to grow for 2h, after which, the solution was transferred to a quartz cuvette and exposed to UV-light (254 nm) for 15 min at room temperature under stirring and further diluted to a final concentration of 1 mM. The sample vitrification procedure was carried out using an automated vitrification robot (FEI VitrobotTM Mark III). CryoTEM grids, R2/2 Quantifoil Jena grids, were purchased from Quantifoil Micro Tools GmbH. Prior to the vitrification procedure (3 μL aliquots, 4 s blotting time, -2 mm blotting offset, 100 % relative humidity) the grids were surface plasma treated using a Cressington 208 carbon coater operating at 5 mA for 40 s. The cryo-TEM experiments were performed on a FEI Technai 20, type Sphera (www.cryotem.nl). The Technai 20 is equipped with a LaB6 filament operating at 200 kV and the images were recorded using a 1k x 1k Gatan CCD camera.

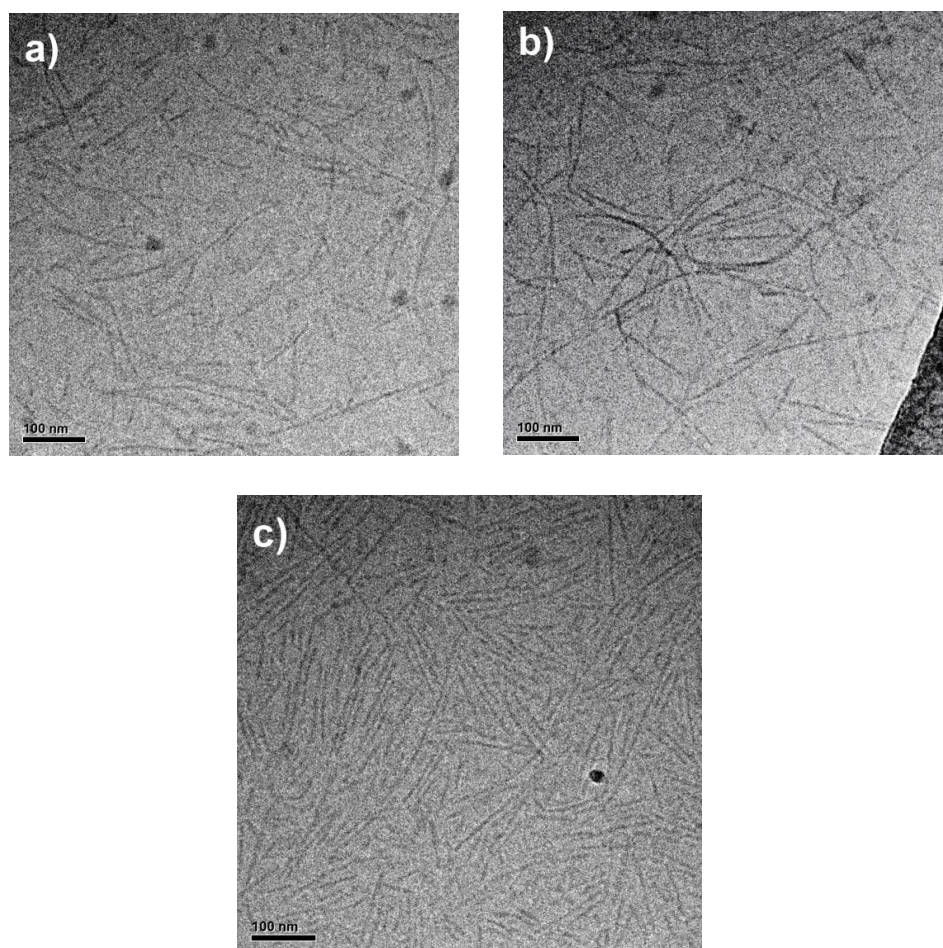


Figure S5. Cryo-TEM micrographs of 1 mM polymerized **PDA** solutions in water.

To calculate L_c and l_p , the above micrographs were first processed using Fiji,^[5] whereby the background of the images was inverted and the high frequency noise smoothed using a Gaussian blur filter. The calculation of L_c distribution was done using the Curve Tracing plugin from Fiji wherein a total sample of 84 micelles was subjected to statistical analysis. Likewise, the calculation of l_p was performed using Easyworm.^[6]

5. UV-Vis spectrum of PDA

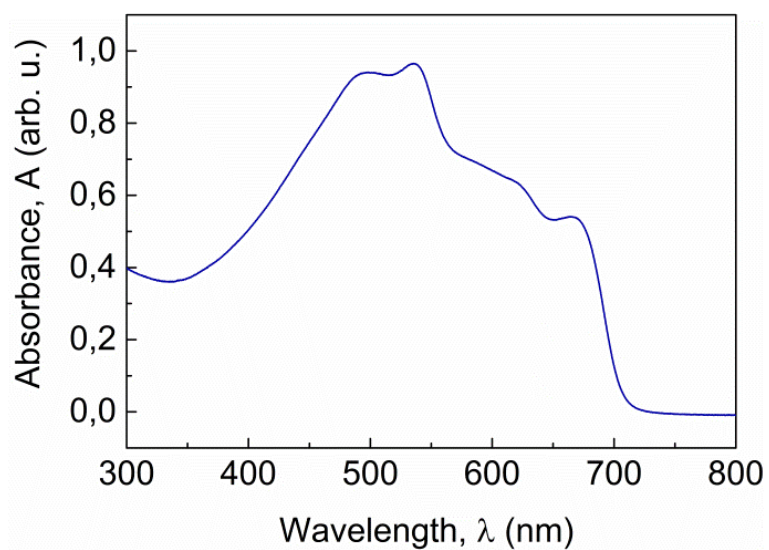


Figure S6. UV-Vis spectrum of **PDA** (0.5 mM) in water. The polymerization was conducted at a concentration of 20 mg mL^{-1} **DA** by exposing the solution to UV-light (254 nm) for 15 min.

6. Calculation of number of ribbons per fiber

Small angle X-Ray scattering was used to determine the number of ribbons per fiber of pre-polymerized self-assembled **PDA** rods. Density measurements of water and **PDA** aqueous solutions were performed on an Anton Paar DMA 5000M.

First, the specific volume (v) of **PDA** rods at a concentration of 10 mg mL^{-1} was determined by measuring the density (D) of **PDA** aqueous solutions over the concentration range indicated in Figure S7:

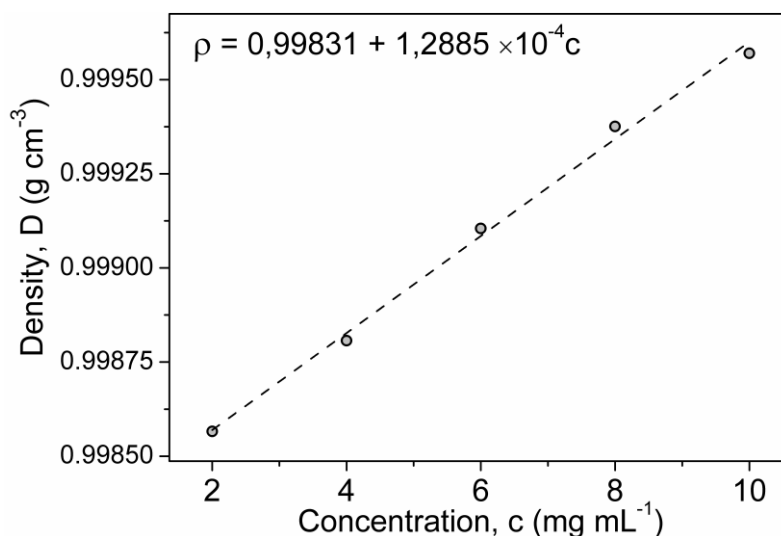


Figure S7. Density of PDA solutions in mili-Q water measured at 20 °C

Thus, the density of a 0.01 g cm^{-3} **PDA** aqueous solution was calculated to be $D_{\text{PDA}}=0.99960 \text{ g cm}^{-3}$. The specific volume was then obtained as:

$$v = \frac{1}{D_{\text{water}}} \left(1 - \frac{D_{\text{PDA}} - D_{\text{water}}}{c} \right) = \frac{1}{0.99820 \text{ g cm}^{-3}} \left(1 - \frac{0.99960 - 0.99820 \text{ g cm}^{-3}}{0.01 \text{ g cm}^{-3}} \right) = 0.86205 \text{ cm}^3 \text{ g}^{-1}$$

In order to fit the experimental data with a non-linear least squares procedure implemented in Igor Pro, we employed a model that calculates the form factor of a flexible cylinder with a uniform scattering length density (ρ_{cyl}) and cross-sectional radial polydispersity which is averaged over a Schultz distribution of cylinder radii. The non-negligible diameter of the cylinder is included by accounting for excluded volume interactions within the walk of a single cylinder. Inter-cylinder interactions are not included.

We then proceeded to fix the values of volume fraction ($\phi = 0.00862$) and use the values of contour length ($L_c = 157 \text{ nm}$) and Kuhn length ($b = 2 \times l_p = 560 \text{ nm}$) as derived from cryo-TEM analysis. The tabulated value of $\rho_{\text{water}} = 9.37 \times 10^{10} \text{ cm}^{-2}$ was used.

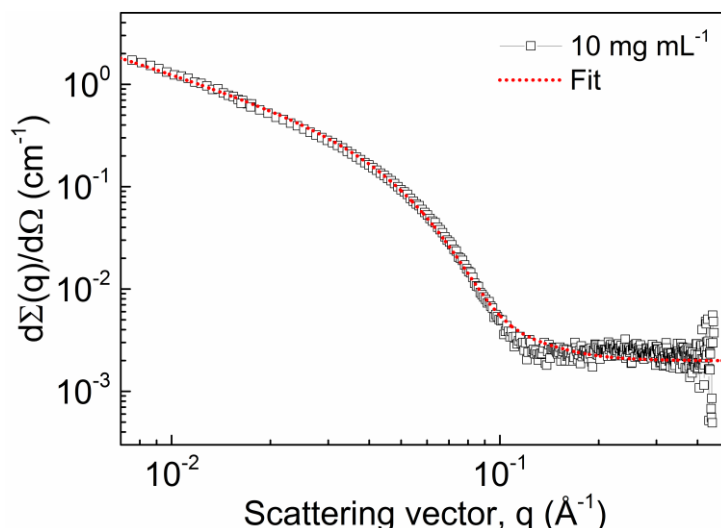


Figure S8. Small angle X-Ray profile (black squares) and form factor fit (red line) of **PDA** solution in milli-Q water recorded at a concentration of 10 mg mL⁻¹.

Fitting of the scattering data with the model (Figure S8) gave a value of 3.1 ± 0.1 nm for the radius, consistent with the value of 3.3 nm measured in cryo-TEM. The fitting procedure also provided a value for $\rho_{\text{cyl}} = (10.43 \pm 0.01) \times 10^{10} \text{ cm}^{-2}$. The scattering contrast was then calculated as:

$$\Delta\rho = \rho_{\text{cyl}} - \rho_{\text{water}} = (10.43 - 9.37) \times 10^{10} \text{ cm}^{-2} = 1.06 \times 10^{10} \text{ cm}^{-2}$$

The electron length density difference ($\Delta\rho_M$) can be now determined as:

$$\Delta\rho_M = \Delta\rho \times v = 1.06 \times 10^{10} \text{ cm}^{-2} \times 0.86 \text{ cm}^3 \text{ g}^{-1} = 9.12 \times 10^9 \text{ cm g}^{-1}$$

The overall scattered intensity for elongated scatterers originates from two separate contributions: A part arising from the cross-section ($I_{\text{cs}}(q)$) and a part resulting from the elongated structure. To calculate the cross-sectional mass per unit length (M_L) we used a Cassasa-Holtzer plot of the data and extrapolated the curve with the parameters obtained from the fitting procedure (Figure S9). This gave the height of the plateau as indicated by the value of the product $[d\Sigma(q)/d\Omega] \times q = 1.23 \times 10^6 \text{ cm}^{-2}$.

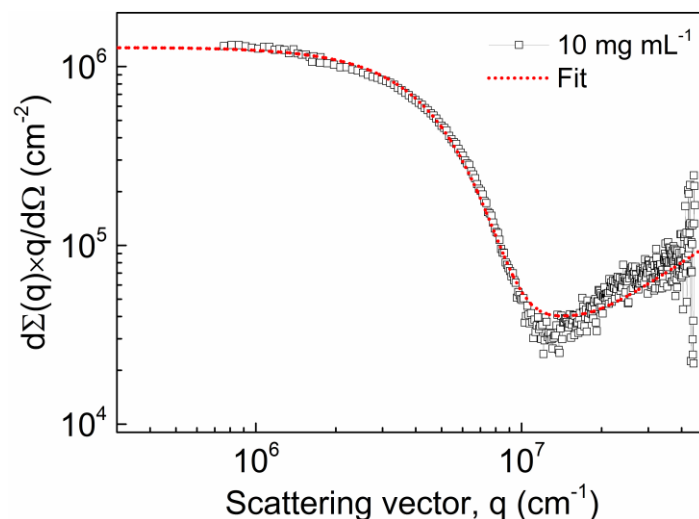


Figure S9. Casassa-Holtzer plot of the scattering profile of **PDA** at 10 mg mL^{-1} . The value of the Holtzer plateau obtained by extrapolation of the experimental data with the best fit parameters as indicated by the dashed red line.

Now, the cross-sectional scattered intensity ($I_{cs}(0)$) was calculated according to the following expression:

$$I_{cs}(0) = \frac{[d\Sigma(q)/d\Omega] \times q}{\pi} = 3.91 \times 10^5 \text{ cm}^{-2}$$

M_L was subsequently obtained using the equation below:

$$M_L = \frac{I_{cs}(0)}{C \times (\Delta\rho_M)^2} = \frac{3.91 \times 10^5 \text{ cm}^{-2}}{0.01 \text{ g cm}^{-3} \times (9.12 \times 10^9 \text{ cm g}^{-1})^2} = 4.70 \times 10^{-13} \text{ g cm}^{-1}$$

Finally, an estimate for the number of ribbons per fiber can be obtained assuming that the distance between molecules along the fiber axis is determined by the repeat distance of the urea-urea hydrogen bonding motif:

$$\begin{aligned} \frac{\text{Molecule}}{\text{H-H}} &= \frac{\text{H-H}_{\text{distance}} \times M_L \times N_A}{M_w} = \frac{4.6 \times 10^{-8} \text{ cm} \times 4.70 \times 10^{-13} \text{ g cm}^{-1} \times 6.02 \times 10^{23} \text{ mol}^{-1}}{1350.9 \text{ g mol}^{-1}} = \\ &= 9.6 \text{ molecules} \end{aligned}$$

$\text{H-H}_{\text{distance}}$ being the distance between urea groups along the stack, N_A Avogadro's number and M_w the molecular weight of **DA**.

7. Gel preparation method

Samples were prepared by weighing **DA** along with **DA-Ac** or **DA-N₃** (10 mol%) in the solid state followed by the addition of ca. 300 μ L chloroform. The resultant solutions were allowed to evaporate overnight. The remaining solid was subsequently redissolved in mili-Q water assisted by applying combined cycles of sonication (30 min) and vortex (1 min) until full dissolution of the solid material. The micelles were then allowed to grow for additional 2 h and the solutions transferred to quartz cuvettes (1 \times 1 cm) followed by exposure to UV-light (254 nm) for 15 min at room temperature under stirring. Equal volumes of polymerized **PDA/DA-Ac** and **PDA/DA-N₃** mixtures were mixed ensuring equimolar acetylene/azide ratios with subsequent addition of premixed aqueous solutions of CuSO₄/Tris(3-hydroxypropyltriazolylmethyl)amine (THPTA) and sodium ascorbate (Na-Ascorbate) to a final concentration of 0.1, 0.5 and 10 mM respectively. The reaction mixture was then immediately transferred to the rheometer where gelation was monitored by oscillatory rheology.

8. Effect of Cu^{I} ions on gelation process

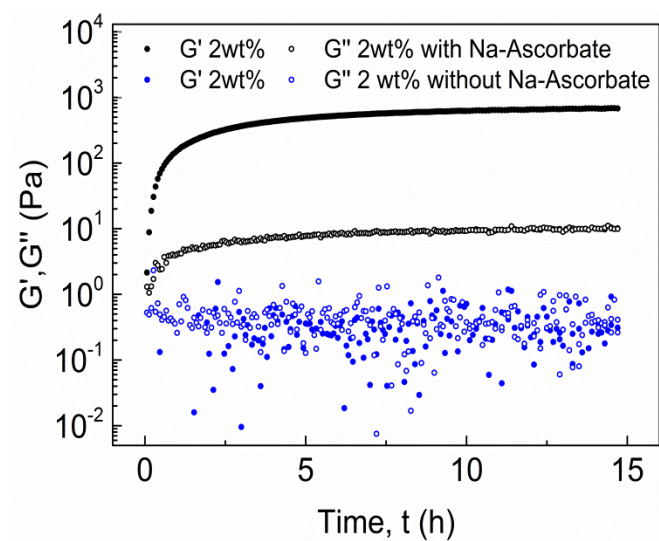


Figure S10. Time sweep experiments for 2 wt% **PDA** co-assembled with 5 mol% **DA-N₃** measured at constant strain amplitudes (0.1 %) and angular frequencies (6.28 rad/s) showing the evolution of G' (solid dots) and G'' (open dots) moduli over time in the presence (black dots) and absence (blue dots) of Na-Ascorbate

9. Scaling relationships and crosslinking length determination

In order to establish the origins of the observed nonlinear elastic response, we have plotted individually the scaling of the plateau modulus (G_0) and the critical stress (σ_c) with concentration; see Figure S11 (a) and (b). In both cases, the double-logarithmic plots clearly reveal two regimes; below the 15 mg/ml concentration point, the dependence of either quantity on concentration is different from that above 15 mg/ml. In addition, the observed power laws are far stronger than those generically expected for semi-flexible polymers. This we attribute to the short, stiff rods in our system combined with the high density. As far as we are aware, no generic scaling prediction exist for this regime.

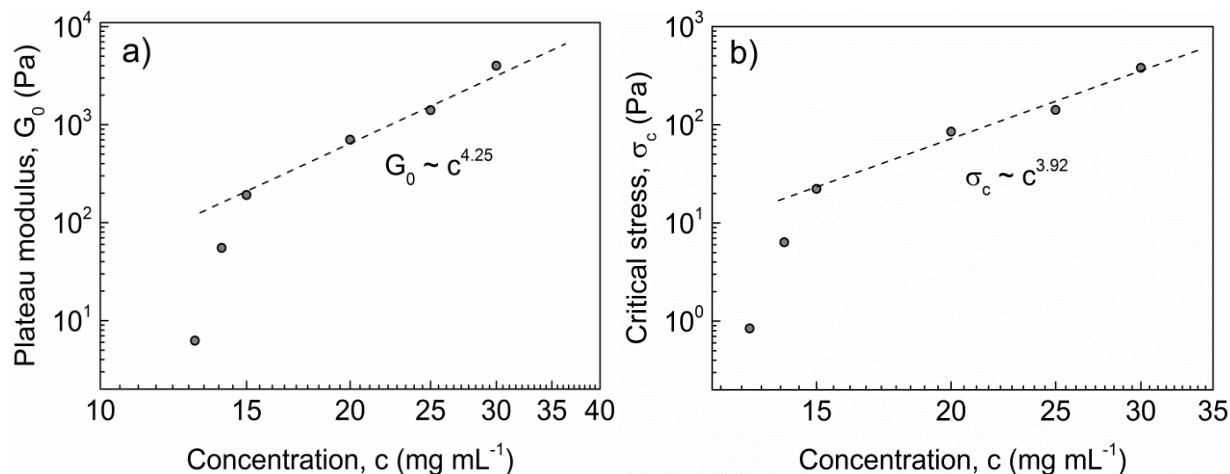


Figure S11. a) Dependence of G_0 on concentration showing two regimes, separated at c of about 15mg/ml dropping the point at 10 mg/mL. b) σ_c vs concentration with two distinct regimes, separated at c of about 15mg/mL dropping the point at 10 mg/mL.

The distinct high- and low density regimes might appear to make it all the more surprising that the nonlinear curves do collapse, but this is incorrect; the values of σ_c and G_0 were chosen such that the rheology curves collapse, and therefore the two observations are not independent. The universal powerlaw $m=1$ at high strains is, however, independent. The fact that it is preserved in both the low- and high density regime suggests a common, strain-prompted nonlinear origin of the stiffening.

Remarkably, across the range of concentrations considered, there is a universal interdependency among concentration, G_0 and σ_c . Following the suggestions in Yao *et al*^[7], we plot in Figure S12 the square root of concentration times the modulus versus the critical concentration, and find - over more than two decades of scaling - a power law relation with a slope very close to 3/2, observed and predicted for intermediate filaments.^[7]

The crosslinking length for the material was estimated by generating coarse-grained networks of stiff rods with a length of 152 nm, and determining how many of the putative crosslinking groups are within crosslinking distance (12nm) of each other, assuming a random arrangement. While we find that for the high volume fractions (4%) of these systems a significant fraction of all crosslinks is expected to be engaged, these links have a strong tendency to cluster around sites of particularly close rod proximity. On average, we estimate from these simulations that 2-3 such clustered connections exist per rod (see Fig S12), which brings the crosslinking length estimate to 50-80 nm

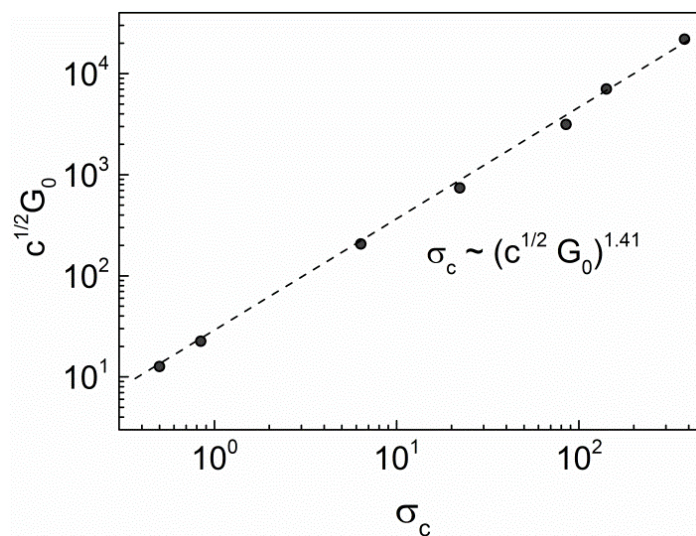


Figure S12. Dependence of $c^{1/2}G_0$ on σ_c . The dashed line is the result of a regression fit to the data and depicts an exponent of 1.41. The scaling appears to be in agreement with the affine thermal model, which predicts an exponent of 3/2.

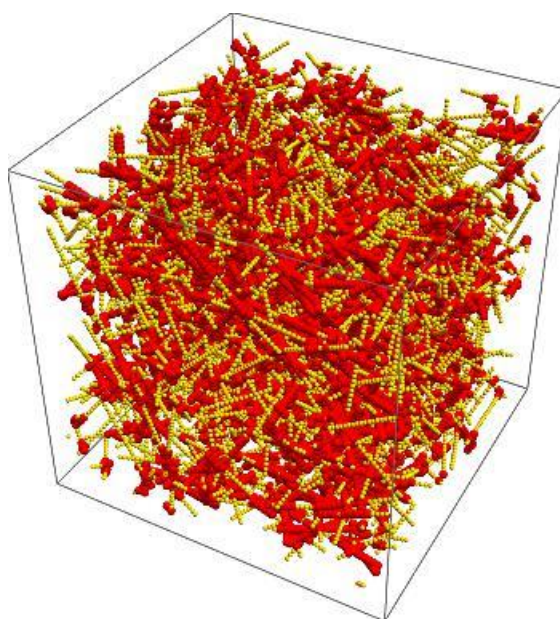


Figure S13. A sample simulated network configuration: 1500 rods of length 152 nm and diameter 6.6 nm in a 500x500x500nm box. Volume fraction (after deleting segments outside of the box) is 3.7%. For this network, 54% of all available crosslinking sites is within crosslinking distance (12nm, sites colored red) of another site, and 2-3 clusters of links occur per rod.

10. References

- S1 L. N. Goswami, Z. H. Houston, S. J. Sarma, S. S. Jalisatgi, M. F. Hawthorne, *Org. Biomol. Chem.* **2013**, *11*, 1116–1126.
- S2 A. Baral, S. Roy, A. Dehsorkhi, I. W. Hamley, S. Mohapatra, S. Ghosh, A. Banerjee, *Langmuir* **2014**, *30*, 929–936.
- S3 A. Pal, P. Voudouris, M. M. E. Koenigs, P. Besenius, H. M. Wyss, V. Degirmenci, R. P. Sijbesma, *Soft Matter* **2014**, *10*, 952–956.
- S4 G. R. Fulmer, A. J. M. Miller, N. H. Sherden, H. E. Gottlieb, A. Nudelman, B. M. Stoltz, J. E. Bercaw, K. I. Goldberg, *Organometallics* **2010**, *29*, 2176–2179.
- S5 J. Schindelin, I. Arganda-Carreras, E. Frise, V. Kaynig, M. Longair, T. Pietzsch, S. Preibisch, C. Rueden, S. Saalfeld, B. Schmid, et al., *Nat. Methods* **2012**, *9*, 676–682.
- S6 G. Lamour, J. B. Kirkegaard, H. Li, T. P. Knowles, J. Gsponer, *Source Code Biol. Med.* **2014**, *9*, 16.
- S7 N. Y. Yao, C. P. Broedersz, Y.-C. Lin, K. E. Kasza, F. C. MacKintosh, D. A. Weitz, *Biophys. J.* **2010**, *98*, 2147–2153.